Thermochimica Acta, 96 (1985) 69–79
Elsevier Science Publishers B.V., Amsterdam – Printed in The Netherlands

OXYGEN CHEMISORPTION BY AN ANTHRACITE FROM PEÑARROYA (SPAIN). A COMPARATIVE STUDY USING DYNAMIC AND ISOTHERMAL GRAVIMETRIC METHODS

C. VALENZUELA CALAHORRO, A. BERNALTE GARCÍA, M. MARTÍNEZ GALLEGO and M.C. FERNÁNDEZ GONZÁLEZ

Department of Inorganic Chemistry, Faculty of Sciences, University of Extremadura, Badajoz (Spain)

(Received 4 June 1985)

ABSTRACT

The chemisorption of oxygen ($P = 1$ atm, flow rate, 200 ml min^{-1}) by an anthracite from Peñarroya and on other adsorbents prepared from the starting sample has been studied in isothermal and dynamic conditions using gravimetric methods.

Hypotheses to justify the thermograms have been established and comparative information on the energetic aspects determining both gasification stages has been obtained.

Some kinetic and thermodynamic aspects are studied from oxygen chemisorption isotherms.

INTRODUCTION

For a century the chemisorption of oxygen on the surface of coal has been well known [1]. Rhead and Wheeler [2,3] suggest that oxygen combines with carbon to form a physico-chemical complex of variable composition, C_xO_y. This complex decomposes upon heating giving a mixture of CO and CO_2.

In recent years, the kinetics and mechanism of oxygen chemisorption on carbonaceous materials have received much attention [4–7].

The amount of oxygen chemisorbed per unit mass of coal depends on the nature of the coal and on temperature, as well as oxygen pressure. On the other hand, the acid–basic character of the complexes formed depends on the experimental conditions in which they were obtained, with the generally accepted rule that when carbon is exposed to oxygen at temperatures between 200 and 500°C, acidic surface oxides are formed [8].

The thermogravimetric study of oxygen chemisorption on an anthracite supplied by Encasur from Peñarroya (Spain) shows that the chemisorption process takes place in the temperature interval $130 \leqslant T \leqslant 400$°C operating both in dynamic (heating rate, 5°C min^{-1}) and isothermal conditions.

The oxygen chemisorption process has been studied and results are given in this report.

0040-6031/85/$03.30

EXPERIMENTAL

The as-received anthracite (A-O) from the mine of Encasur in Peñarroya (Córdoba, Spain) and the following samples were used: A-H (by treatment of A-O with 5 N HCl; A-N (by treatment of A-H with 2 N HNO_3); A-F (by treatment of A-H with 45% HF); and A-C (by carbonization of A-O at 1000°C, 10°C min^{-1}, and an isothermal treatment of 2 h), all identified elsewhere [9].

In all cases, the particle size used was between 0.150 and 0.200 mm.

The A-O, A-H, A-N, A-F and A-C surface areas were determined by N_2(g) (at 77 K) and CO_2(g) (at 273 K) adsorption using, respectively, a volumetric and a gravimetric apparatus for gas adsorptions.

The chemisorption of oxygen in a dynamic atmosphere created by such a gas (flow rate, 200 ml min^{-1}; $P = 1$ atm) was studied both in dynamic ($130 \leqslant T \leqslant 400$°C; heating rate, 5°C min^{-1}) and isothermal (250, 275 and 300°C) conditions.

Previously, in all cases, samples were heated up to 250°C (N_2, flow rate, 200 ml min^{-1}; heating rate, 10°C min^{-1}) in order to eliminate the hydration water, and subsequently up to the final operating temperature.

RESULTS AND DISCUSSION

Table 1 shows data for the adsorbents, which were discussed in a previous report, to be published soon [9].

The chemisorption of oxygen was observed only in three adsorbents (A-O, A-H and A-F) whereas the other samples (A-N and A-C) do not adsorb this gas significantly.

When operating in dynamic conditions, we obtained the results shown in Fig. 1 in which it is observed that the amount of oxygen chemisorbed, X (mol O_2/g dried adsorbent) presents a significant value only above 130°C for A-O and A-H and above 220°C for A-F. The X value increases up to a

TABLE 1

Surface areas (N_2, 77 K and CO_2, 273 K)

Sample	Ash (%)	S (m^2 g^{-1})		
		N_2 (BET)	N_2 (Langmuir)	CO_2 (Langmuir)
A-O	37.46	12.7	14.4	67.0
A-H	32.41	22.4	31.3	66.3
A-N	28.67	21.8	25.0	66.4
A-F	9.99	30.3	27.6	104.3
A-C	50.25	3.2	3.7	13.9

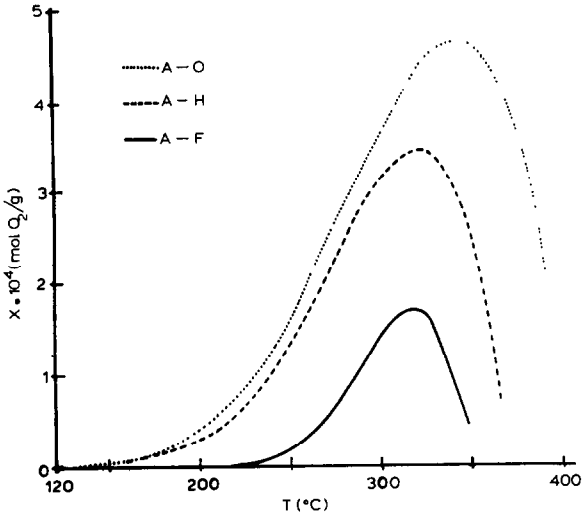

Fig. 1. Chemisorption of oxygen in dynamic conditions.

maximum and after that decreases on increasing temperature. Such curves are found to be similar to those obtained by Bradbury and Shafizadeh when investigating the chemisorption of oxygen on cellulose char [10].

The curves in Fig. 1 can be explained by considering that the combustion process occurs after a mechanism, which implies the previous chemisorption of oxygen to form CO_z and the subsequent decomposition of this intermediate species giving CO(g) or CO_2(g) according to

$$C(s) + O_2(g) \underset{k_2}{\overset{k_1}{\rightleftharpoons}} CO_z(s) \begin{cases} \xrightarrow{k_3} CO_2(g) \\ \xrightarrow{k_4} CO(g) \end{cases} \quad (1)$$

As CO_2(g) formation, in thermodynamic terms, is more favourable than CO(g) formation for $T \leqslant 710°C$, and we have operated in the temperature interval 130–400°C in an excess of oxygen, it can be considered that only CO_2(g) is formed during CO_z decomposition. Thus, we suppose that the overall process takes place in two stages: one of chemisorption

$$C(s) + O_2(g) \underset{k_2}{\overset{k_1}{\rightleftharpoons}} CO_z(s) \quad (2)$$

and another of decomposition

$$CO_z(s) \xrightarrow{k_3} CO_2(g) \quad (3)$$

Considering both stages separately, the first must give rise to a weight gain of the starting sample. On the contrary, the second stage would bring about a weight loss in relation to the maximum value, which corresponds to the largest amount of CO_z formed.

For a system at equilibrium conditions with $P_{O_2} = 1$ atm and conversion degree, α, the equilibrium constant is given by

$$K_1 = K_p P_{O_2} = \frac{12}{12 + 16z} \cdot \frac{\alpha}{1 - \alpha} \tag{4}$$

As the maximum amount of chemisorbed O_2 is about 10^{-3} mol O_2/g adsorbent, it can be considered that $1 - \alpha = 1$ and, hence

$$K_1 = \frac{12}{12 + 16z}\alpha \tag{5}$$

The unitary increase of the carbon mass is given by

$$\Delta m = \frac{4z}{3}\alpha \tag{6}$$

Substituting the α value deduced from eqn. (5) in eqn. (6), we obtain

$$\Delta m = \frac{4z}{3}\left(1 + \frac{4z}{3}\right)K_1 \tag{7}$$

and when Δm is considered as moles of O_2 chemisorbed per gram of carbon

$$X = \frac{\Delta m}{32} = \frac{z}{24}\left(1 + \frac{4z}{3}\right)K_1 = \frac{z}{24}\left(1 + \frac{4z}{3}\right)\exp(\Delta S_1/R)\exp(-\Delta H_1/RT) \tag{8}$$

If ΔH and ΔS remain constant within the temperature interval considered, the plot of ln X vs. $1/T$ must give rise to a straight line.

In the same way, for process (3) and considering β as the conversion degree

$$K_2 = \frac{12 + 16z}{44} \cdot \frac{\beta}{1 - \beta} \approx \frac{12 + 16z}{44}\beta \tag{9}$$

The weight decrease ($\Delta m'$) in relation to the maximum value (m_{max}) is given by

$$\Delta m' = m_{max}\beta = m_{max}\frac{44}{12 + 16z}K_2 \tag{10}$$

and when $\Delta m'$ is considered as moles of O_2 (equal to moles of CO_2) desorbed per gram of initial sample (X')

$$X' = \frac{11 m_{max}}{8(12 + 16z)}\exp(\Delta S_2/R)\exp(-\Delta H_2/RT) \tag{11}$$

Obviously, eqns. (8) and (11) are only valid for equilibrium states and temperature intervals in which ΔH and ΔS can be considered constant. Nevertheless, if we operate in dynamic conditions at a low heating rate, the experimental results can follow such equations; however, in such a case, ΔH and ΔS will be only comparative values.

In the present case, the results in Fig. 1 have been plotted as log X vs. $1/T$ (Fig. 2), and it can be observed that such data follow eqns. (8) and (11).

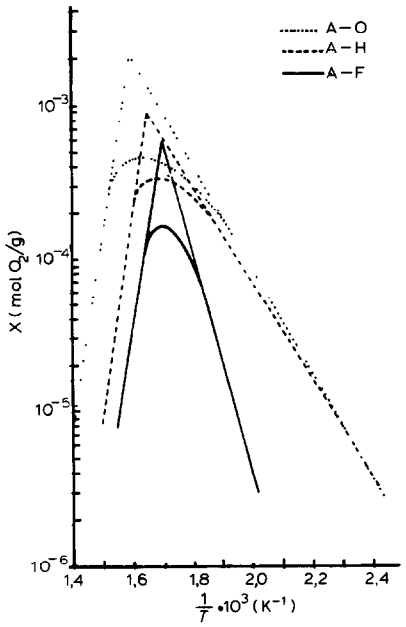

Fig. 2. Application of eqns. (8) and (11) to the experimental results given in Fig. 1.

On the other hand, once the least-squares method is applied, the slope and intercept values corresponding to each straight line are determined and the ΔH values deduced from the slope data. Likewise, the determination of X_{max} values, which are given by the intersection point of both straight lines corresponding to each adsorbent, enables us to estimate z_{max} values. These data are all presented in Table 2.

These results suggest that CO_z formation occurs by following an endothermic process. ΔH_1 varies between 14.2 and 33.0 kcal mol^{-1}, and z decreases with the mineral matter content in the adsorbent. It can also be noted that ΔH_2 values are rather close to each other (≈ -60 kcal mol^{-1}), which seems

TABLE 2

Parameter determined by applying eqns. (8) and (11)

Sample	ΔH_1 [a] (kcal mol^{-1})	X_m (mmol O_2/g)	z_1 [b]	z_2 [c]	z_3 [d]	z_4 [e]	ΔH_2 [a] (kcal mol^{-1})
A-O	15.4	2.081	0.025	0.045	0.052	0.10	−57.5
A-H	14.2	0.861	0.010	0.017	0.020	0.04	−64.1
A-F	33.0	0.596	0.007	0.008	0.010	0.02	−56.8

[a] Apparent values.
[b] z_1 = mol O_2/at.g dry sample.
[c] z_2 = mol O_2/at.g dry, ash-free sample.
[d] z_3 = mol O_2/at.g C (dry, ash- and volatile material-free sample).
[e] $z_4 = z$ value in CO_z.

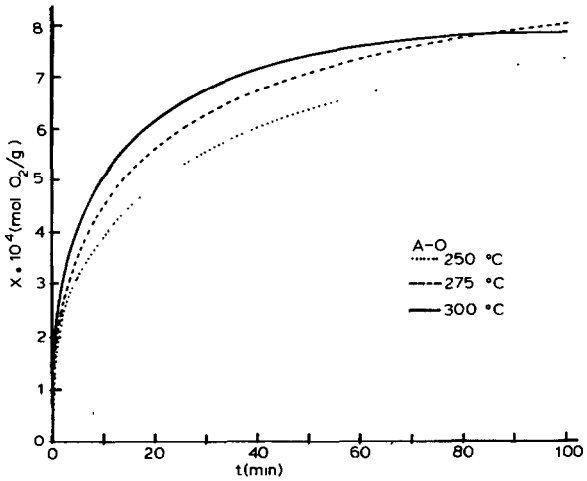

Fig. 3. Chemisorption of oxygen by A-O.

to indicate a smaller influence of the mineral matter on process (3).

Moreover, if we consider that the oxygen is completely chemisorbed to form CO_z-type complexes, the really valid z values will be those shown as z_4 in Table 2 (at.g oxygen/at.g carbon). z_4 constantly presents a smaller value for acid-treated samples than for sample A-O. Thus, as the acid treatments give rise to the opening of open-cavity type pores with diameter ranging between 0.41 and 0.50 nm [11], results suggest that the oxygen complexes are mainly formed at the entrances of such pores because of the greater disorder of the atoms in these regions [12].

As has already been mentioned, eqns. (8) and (9) are rightly applied only to equilibrium states, therefore what has been pointed out above has only a merely comparative interest. For this, the chemisorption isotherms of oxygen

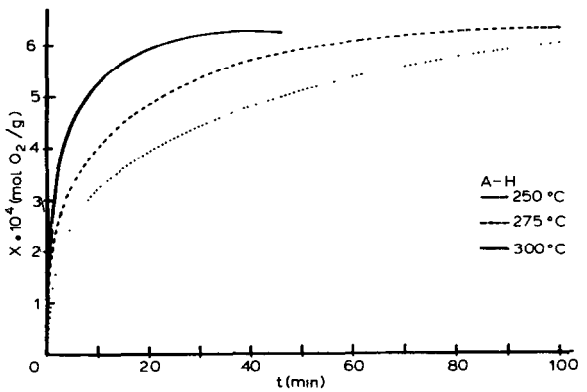

Fig. 4. Chemisorption of oxygen by A-H.

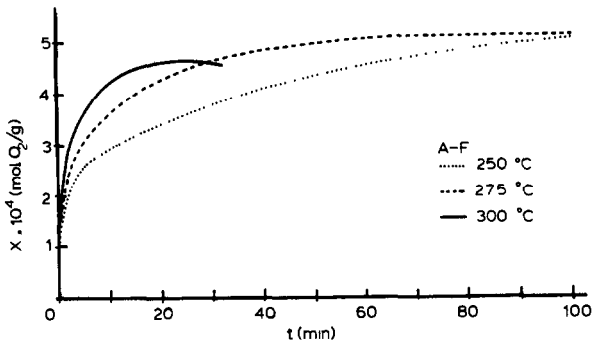

Fig. 5. Chemisorption of oxygen by A-F.

for A-O, A-H and A-F have been obtained at 250, 275 and 300°C and the results are presented in Figs. 3–5, respectively.

The isotherms for A-H and A-F show a maximum value at 300°C and the amount chemisorbed decreases thereafter due to the prevalence of CO_z decomposition, giving CO_2, on O_2(g) chemisorption. The isotherms at 250 and 275°C do not reach such a maximum value.

All the experimental isotherms follow an equation of the type

$$X = \frac{X_m C t^n}{1 + C t^n} \tag{12}$$

where X_m represents the chemisorption capacity of O_2 (mol g^{-1} dry matter), C is a constant related to the equilibrium constant and n is the reaction order with regard to time or the apparent order of Letort [13].

As eqn. (12) is similar to Koble and Corrigan's equation [14], it has been solved in the usual manner by determining X_m (Table 2) and then plotting log $X/(X_m - X)$ vs. log t, the resulting straight lines, once fitted by the

TABLE 3

Parameters of eqn. (12)

Sample	T (°C)	X_m (mmol g^{-1})	C	n	r
A-O	250	1.75	0.113	0.412	0.9997
	275	1.35	0.161	0.491	0.9995
	300	1.10	0.245	0.545	0.9996
A-H	250	1.50	0.112	0.390	0.9998
	275	0.99	0.262	0.430	0.9991
	300	0.75	0.600	0.604	0.991
A-F	250	1.50	0.125	0.299	0.9968
	275	0.90	0.276	0.386	0.9995
	300	0.55	0.670	0.665	0.9999

TABLE 4

Apparent orders, specific rate and thermodynamic magnitudes of activation

Sample	T (°C)	n_1	n_2	k	ΔH^* (kcal mol^{-1})	ΔS^* (cal mol^{-1} K^{-1})
A-O	250	3.43	−1.43	1.18	40.1	17.5
	275	3.04	−1.04	8.82		
	300	2.83	−0.83	37.58		
A-H	250	3.56	−1.56	0.95	69.1	72.3
	275	3.33	−1.33	19.28		
	300	2.66	−0.66	345.68		
A-F	250	4.34	−2.34	0.19	96.0	120.7
	275	3.59	−1.59	15.27		
	300	2.50	−0.50	662.09		

method of least squares, present linear correlation coefficients, r, close to one (Table 3). The slope and intercept for each straight line enable us to calculate, respectively, n and C values, which are given in Table 3.

X_m decreases when temperature is increased, similar to CO_z thermodynamic stability. Moreover, the order with regard to time, n, presents in all cases a value close to 0.5 which increases with temperature.

From eqn. (12) the following kinetic equation can be easily deduced

$$\frac{dX}{dt} = \frac{nC^{1/n}}{X_m}(X_m - X)^{(n+1)/n} X^{(n-1)/n} = k(X_m - X)^{n_1} X^{n_2} \tag{13}$$

This equation corresponds to an irreversible process, in good agreement with the experimental results of the thermal decomposition of CO_z(s) producing CO_2(g) or CO(g) [4].

The values of the specific rate, k, as well as the apparent orders are given in Table 4; k increases, as might be expected, with temperature, while n_1 (> 0) and n_2 (< 0) decrease in absolute value when temperature is increased, confirming that they are not true orders but only apparent orders.

The activation enthalpies, ΔH^*, and entropies, ΔS^*, of the CO_z formation process have been analytically calculated (Fig. 6) from k values. The results suggest that the formation of the corresponding activated species is so unlikely, since the original sample has a greater carbon content. $\Delta S^* > 0$ might be explained by supposing a possible decrease in the bond order in the carbon–carbon links due to the π- and even σ-bond breakings, which would bring about a significant increase in the degrees of freedom of the elementary crystallites of the graphite constituents of carbon.

Considering the nature of this chemisorption process, it is obvious that oxygen diffusion inside the particles of carbon must have a great influence on such a process. For this reason, the experimental results from the kinetic

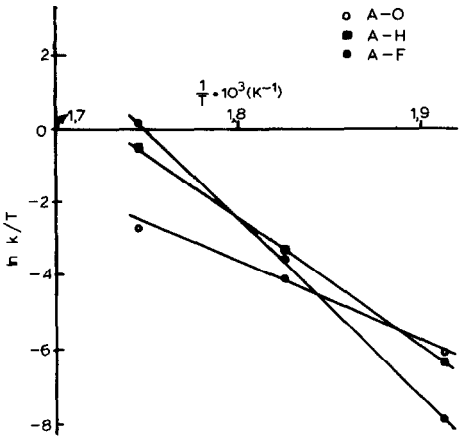

Fig. 6. Arrhenius plot. Thermodynamic magnitudes of activation.

study have been utilized as a starting point to gain information on the influence of the diffusion stage on the overall process of chemisorption. Such a diffusion process must be approximately governed by the resulting equation when the mathematical expression of Fick's second law [15] is integrated for a sphere of radius a

$$\frac{C_t - C_0}{C_1 - C_0} = 1 + 2\sum_{n=1}^{\infty}(-1)^n \exp(-Dn^2\pi^2 t/a^2) \tag{14}$$

Due to the way we have worked, for $t = 0$ inside the adsorbent and $C_0 = 0$, for small t values eqn. (14) can be written as

$$\frac{C_t}{C_1} = \frac{a}{r}\sum_{n=0}^{\infty}\left[\mathrm{ERFC}\frac{(2n+1)a - r}{2Dt} - \mathrm{ERFC}\frac{(2n+1)a + r}{2Dt}\right] \tag{15}$$

where C_t represents the concentration at time t (s) inside the particle, C_1 the concentration in contact with the particle, D the diffusion coefficient ($cm^2\ s^{-1}$), a the radius of the sphere (cm), r the distance to the point under consideration, and ERFC the error function complement.

In this case, considering the particles as approximately spherical of average diameter 0.180 mm and with densities of 1.72 g cm^{-3} for A-O, 1.64 cm^{-3} for A-H and 1.45 g cm^{-3} for A-F, at $t = 10$ min and $r/a = 0.5$, we have obtained the diffusion coefficient values shown in Table 5. They are close to 10^{-9} $cm^2\ s^{-1}$ and increase with temperature.

From the diffusion coefficients and considering [16]

$$D = D_0 \exp(-E_a/RT) \tag{16}$$

one can estimate the frequency factors, D_0, and the activation energy for the diffusion process (Table 5). D_0, the value for D when $T = \infty$, is about 10^{-9} $cm^2\ s^{-1}$ and the activation energies, E_a, close to 1 kcal mol^{-1}.

On the other hand, X_m values (Table 3) have been analysed by eqn. (8) by

TABLE 5

Diffusion coefficients, frequency factors and activation energies

Sample	T (°C)	$D \times 10^9$ ($cm^2\ s^{-1}$)	$D_0 \times 10^9$ ($cm^2\ s^{-1}$)	E_a (kcal mol^{-1})
A-O	250	2.81	7.26	0.98
	275	2.93		
	300	3.05		
A-H	250	2.69	10.89	1.46
	275	2.82		
	300	3.04		
A-F	250	2.59	6.16	0.90
	275	2.70		
	300	2.80		

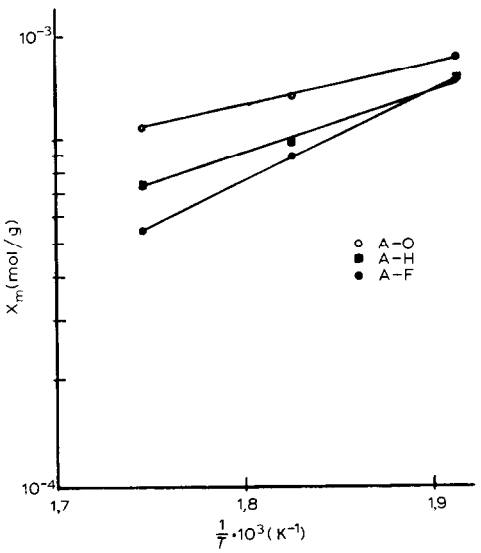

Fig. 7. Application of eqn. (8) to obtained X_m values.

TABLE 6

Thermodynamic magnitudes of the chemisorption process of oxygen

Sample	ΔH_1 (kcal mol^{-1})	ΔS_1 (cal $mol^{-1}\ K^{-1}$)	r
A-O	−5.5	−14.2	0.9990
A-H	−8.3	−17.6	0.9959
A-F	−11.9	−23.1	0.9998

plotting log X_m vs. $1/T$ (Fig. 7) and from the resulting straight lines, once analysed by the method of least squares, ΔH and ΔS (Table 6) have been obtained. It can be deduced from these data that oxygen chemisorption takes place by an exothermic and exoentropic process, in good agreement with the formation of C–O bonds, since the number of degrees of freedom of the system decrease due to oxygen retention.

From the results given above, it can be established that thermogravimetric techniques do not furnish comparable information when operating in both dynamic and isothermal conditions, only the latter method can provide adequate information on the oxygen chemisorption process.

REFERENCES

1 R.A. Smith, Proc. R. Soc. London, 12 (1863) 424.
2 T.F.E. Rhead and R.V. Wheeler, J. Chem. Soc., 101 (1912) 846.
3 T.F.E. Rhead and R.V. Wheeler, J. Chem. Soc., 103 (1913) 461.
4 D.L. Carpenter and G.D. Sergeant, Fuel, 45 (1966) 311.
5 D.J. Allardice, Carbon, 4 (1966) 255.
6 R.C. Bansal, F.J. Vastola and P.L. Walker, Jr., J. Colloid Interface Sci., 32 (1970) 187.
7 R.C. Bansal, F.J. Vastola and P.L. Walker, Jr., Carbon, 10 (1972) 443.
8 P.N. Cheremisinoff and F. Ellerbusch (Eds.), Carbon Adsorption Handbook, Ann Arbor Science Publishers, Ann Arbor, MI, 1978.
9 M.C. Fernandez Gonzalez, Tesina de Licenciatura, Fac. Ciencias, Universidad de Extremadura, Badajoz, 1983.
10 A.G.W. Bradbury and F. Shafizadeh, Carbon, 18 (1980) 109.
11 P.L. Walker, Jr., L.G. Austin and S.P. Nandi, Chemistry and Physics of Carbon, Vol. 2, Dekker, New York, 1966.
12 S.P. Nandi, V. Ramadass and P.L. Walker, Carbon, 2 (1964) 199.
13 M. Letort, Bull. Soc. Chim. Fr., (1942) 9.
14 R.A. Koble and T.E. Corrigan, Ind. Eng. Chem., 44 (1952) 383.
15 J. Crank, The Mathematics of Diffusion, Oxford University Press, Oxford, 1956.
16 W. Jost, Diffusion in Solids, Liquids and Gases, Academic Press, London, 1952.